available at www.sciencedirect.com

ScienceDirect

journal homepage: www.ejconline.com

Magnetic resonance spectroscopy suggests key differences in the metastatic behaviour of medulloblastoma

Andrew C. Peet[a,b,*], *Nigel P. Davies*[a,c], *Lee Ridley*[d], *Marie-Anne Brundler*[b], *Dimitris Kombogiorgas*[b], *Shaheen Lateef*[b], *Kal Natarajan*[a,c], *Spyros Sgouros*[b], *Lesley MacPherson*[b], *Richard G. Grundy*[a,b,e]

[a]*Academic Department of Paediatrics and Child Health, University of Birmingham, Whittall Street, Birmingham B4 6NH, UK*
[b]*Birmingham Children's Hospital NHS Trust, Steelhouse Lane, Birmingham B4 6NH, UK*
[c]*Department of Medical Physics, University Hospital Birmingham, Birmingham, UK*
[d]*The Children's Brain Tumour Research Centre, The Medical School, Floor D, University of Nottingham, Nottingham NG7 2UH, UK*

ARTICLE INFO

Article history:
Received 28 November 2006
Accepted 15 January 2007
Available online 8 March 2007

Keywords:
Children
Medulloblastoma
Magnetic resonance spectroscopy
Metastases

ABSTRACT

Background: Metastatic medulloblastoma has a poorer prognosis than localised disease in part due to inherent properties of the tumour. ^{1}H magnetic resonance spectroscopy (MRS) provides a powerful method for investigating tumour metabolism *in vivo*.
Methods: Magnetic resonance imaging and short echo time (Te 30 ms) single voxel MRS were performed on the primary tumour of 16 children with medulloblastoma prior to surgical resection. Tumour volumes were calculated using a segmentation technique and the MRS was analysed using LCModel™.
Results: Patients with metastatic disease had primary tumours which were smaller ($p = 0.01$), had higher levels of total choline ($p = 0.03$) and lower levels of mobile lipids ($p = 0.04$).
Conclusion: Metastatic medulloblastomas have metabolite profiles indicative of increased cell growth and decreased cell death compared with localised tumours reflecting intrinsic differences in underlying biology. Localised tumours with an MRS metabolite profile similar to those with metastatic disease may be at increased risk of metastatic relapse.

1. Introduction

The prognosis for medulloblastoma in children varies widely depending on histology, stage and age at diagnosis. Increasingly it has become clear that prognosis is related to the underlying biology of the tumours and a number of genetic markers have been identified together with their molecular pathways.[1–5] The biological and clinical behaviour of medulloblastomas is determined by the downstream effects of these genetic alterations and it is increasingly apparent that biomarkers which sample downstream effects can also provide useful predictors of outcome. One such method is ^{1}H magnetic resonance spectroscopy (MRS), an imaging modality closely related to MRI, which determines in vivo concentrations of

* *Corresponding author*: Address: Academic Department of Paediatrics and Child Health, University of Birmingham, Whittall Street, Birmingham B4 6NH, UK. Tel.: +44 121 333 8234; fax: +44 121 333 8421.
E-mail address: acpeet@doctors.org.uk (A.C. Peet).
Abbreviation: MRS, ^{1}H magnetic resonance spectroscopy.
[e] Present address: The Children's Brain Tumour Research Centre, The Medical School, Floor D, University of Nottingham, Nottingham NG7 2UH, UK.
0959-8049/$ - see front matter © 2007 Elsevier Ltd. All rights reserved.
doi:10.1016/j.ejca.2007.01.019

metabolites. MRS metabolite profiles have been shown to provide a powerful method for characterising brain tumours.[6,7]

Predicting which children with 'standard' risk Medulloblastoma will fail therapy is of particular clinical import, especially if this can be determined at diagnosis. The development of 'real time' non-invasive biomarkers would be of significant clinical benefit since they also have the potential to allow treatment to be adapted according to the evolving nature of the disease. Furthermore, investigation of the downstream effects of genetic alterations enhances the potential for discovering new targets for drug delivery.

Certain tumour metabolite levels determined by MRS have been shown to provide useful prognostic information. High total choline levels, total choline/creatine ratios and total choline/NAA ratios have been noted as markers of poor prognosis for a number of tumours.[8–12] MRS imaging has also been used to identify the most active regions of brain tumours in adults.[13,14] Myoinositol and mobile lipids levels correlate well with grade in astrocytomas[15] and mobile lipid levels show a correlation with malignancy across a range of paediatric brain tumours.[8,16] Animal studies have shown that choline/mobile lipid ratios in neuroblastoma correlate with the viable tumour fraction and rate of tumour growth.[17]

Increased levels of phosphocholine in particular have been related to ras oncogene activation[18] and increased activity of choline kinase[19] giving potential therapeautic targets.[20] Interest has also focused on lipids visualised by MRS, with high levels noted in necrotic tumours such as grade IV astrocytomas.[13,14] However, mobile lipids have also been associated with apoptosis[21] and *in vitro* studies have identified the accumulation of intracellular lipid droplets in the cells to account for this.[22] The demonstration of mobile lipids on MRS has been associated with metabolic cell stress and loss of viability, but the pathways underlying this process have not yet been fully delineated nor histopathological markers been accurately determined.

Here we test the hypothesis that biologically aggressive medulloblastomas have a characteristic metabolite profile by correlating MRS of the primary tumour with clinical features, histopathology and tumour size.

2. Materials and methods

2.1. Patients

Patients undergoing MR imaging at Birmingham Children's Hospital as part of their clinical investigations for a suspected brain tumour were eligible for entry into the study. Local and multicentre research ethical approval was obtained and informed consent taken from parents/guardians for enrollment.

2.2. Magnetic resonance imaging and spectroscopy protocol

MRI and MRS were carried out on a 1.5 T Siemens Symphony Magnetom. Standard imaging included T1 and T2 weighted images of the brain followed by gadolinium contrast administration and then T1 weighted images of the head and spine. The conventional imaging set was used to delineate the margins of the primary tumour and the voxel for MRS was placed entirely within this region. Point resolved single voxel spectroscopy was performed with an echo time of 30 ms and a repetition time of 1500 ms. Cubic voxels of either 2 cm or 1.5 cm length were used depending on the size of the tumour. Water suppressed MRS data were acquired with 128 repetitions from the larger voxels and 256 repetitions from the smaller ones. Water unsuppressed MRS data were also acquired for eddy current correction and as a reference for calculating concentrations.

Outer volume lipid suppression was not used in this study due to a lack of availability. To ascertain the potential for lipid contamination of the MRS signal from outside the tumour, lipid levels were compared between tumour and a set of controls. The controls consisted of children in remission following treatment for a posterior fossa tumour and MRS was performed on non-involved cerebellum. In all MRS studies, images of voxel placement were saved and the closest point of the voxel to scalp lipid was measured.

2.3. Histopathology

Samples obtained at surgery from all patients were subjected to histopathological examination using standard H&E stains as well as a panel of immunohistochemical stains including synaptophysin and GFAP. Tumour proliferation and apoptosis were determined by immunohistochemical staining with Ki67 (mouse monoclonal antibody, DAKO) and cleaved caspase-3 (*Rabbit polyclonal Ab, Asp 175, Cell Signaling*), using standard techniques. The fraction of viable tumour was estimated by combining the percentage of apoptotic cells as assessed by staining for cleaved caspase-3 and the percentage of tumour necrosis estimated from the H&E stains. The surface area of tumour analysed to determine the viable tumour fraction was noted. Five micrometer sections were obtained from each sample. Following overnight incubation at 37 °C, the sections were dewaxed in xylene and hydrated through lowering concentrations of ethanol. For antigen retrieval, the sections were treated in sodium citrate buffer (pH 6.0) for 1 min at full pressure in a pressure cooker. The sections were blocked for endogenous peroxidase. Incubation of the Ki67 antibody was carried out at 1:50 for one hour at room temperature. Caspase-3 was incubated at 1:400, at 4 °C overnight. Positive Control tissue for Ki67 and caspase-3 were used, including appendix and tonsil, respectively. Detection of the target antigen was carried out using the DAKO Chemate Envision Detection Kit (DAKO, UK) and DAB was used for visualisation of the target antigen. Finally, sections were counterstained with Harris Haematoxylin, dehydrated and mounted for analysis (see Fig. 1).

2.4. Analysis of MR imaging and spectroscopy data

The magnetic resonance imaging and spectroscopy data (including the free induction decay) were transferred to a dedicated Sun Sparc computer server. Tumour volumes were calculated by a segmentation technique employing mostly manual outlining applied on the whole set of 2D axial

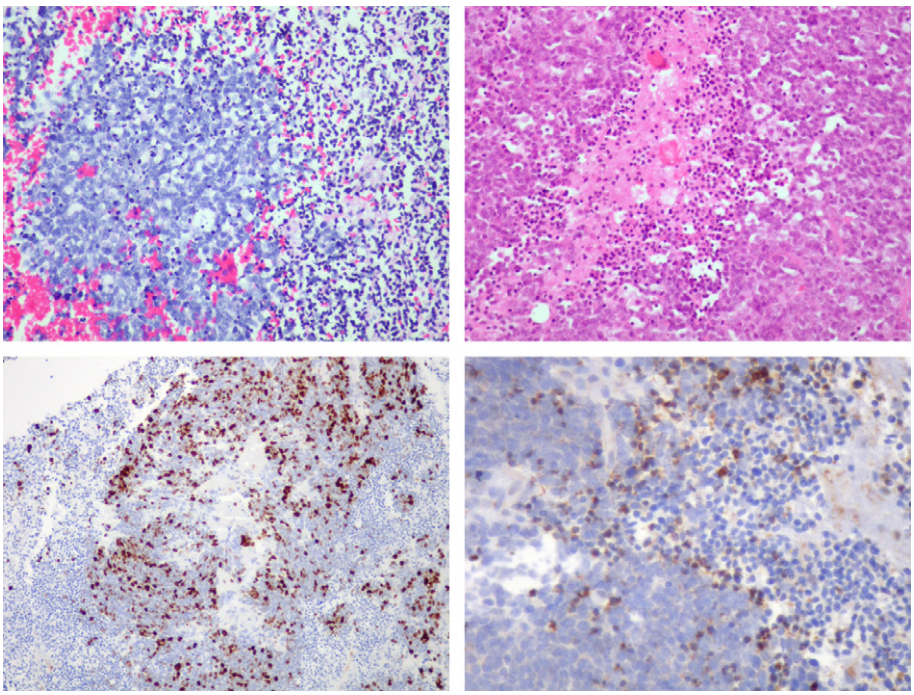

Fig. 1 – a (top left) and b (top right) Haematoxylin Eosin stained sections show classical and large cell medulloblastoma with areas of necrosis (right side of a and centre of b) and apoptosis characterised by nuclear fragmentation. c (bottom left) and d (bottom right) illustrate immunohistochemical staining for proliferation marker Ki67 (nuclear staining), and cleaved Caspase3 (granular cytoplasmic staining), which is one of the key executioners of apoptosis. Note the wedge shaped area of tumour necrosis (right side of d) which remains unstained.

images.[23] For all children, preoperative volumetric axial post-IV-contrast T1-weighted sequences with 1.62 mm thickness were used for tumour measurement. While post-contrast T1-weighted sequences were used to take advantage of the contrast enhancement that most medulloblastomas exhibit, T2-weighted MR images were consulted in parallel, to assist in differentiation between tumour and the surrounding oedema as best as possible. Attention was paid to areas of no or mixed contrast enhancement, to avoid over or under estimating tumour volume. The outlines were performed initially by one observer (DK) and independently verified by a second observer (SS).

The raw MRS signals were processed using the LCModel software package (version 6.0-1),[24] an accurate and reliable method for automatic quantitation of metabolite concentrations from short TE *in vivo* proton MR spectra.[25] LCModel fits the *in vivo* spectrum to a linear combination of individual metabolite spectra obtained under similar conditions from solutions of expected metabolites that make up the basis set. The basis set used contained 16 metabolites and 9 lipid and macromolecular components. Estimated concentrations for each metabolite, lipid and macromolecular component were obtained by reference to a spectrum acquired without water suppression from the same voxel. This reference spectrum was also used to correct for eddy current effects present in the water suppressed spectra. The mean metabolite concentrations obtained from the LCModel analysis were compared between the groups of patients with ($N = 8$) and without metastases ($N = 8$) using a series of two-tailed Student's unpaired *t*-tests.

The processed spectra were extracted from the LCModel analysis to compute average spectra for the metastatic and non-metastatic groups of patients. A principal components anlaysis (PCA) was then performed on the points in the spectra between 0.2 and 4 ppm. The principal component analysis generates a plot in which the axes are chosen to encapsulate the maximum amount of variance in the data without imposing any prior knowledge about the data. Each spectrum is represented in the plot by a point and similar spectra cluster together. This method of representing the data allows the amount of variability and similarity in the spectra to be visualised.

3. Results

3.1. *Patient characteristics*

Twenty patients were diagnosed with medulloblastoma between 1st September 2003 and 1st October 2005. At the time of MRI and MRS, none of the patients had undergone surgery to their tumour or received previous chemotherapy or radiotherapy. Data from 4 patients were not eligible (80% accrual), 3 did not have MRS performed prior to surgery and the other patient had MRS of a large metastatic lesion where the primary tumour was small. All patients underwent MRI of the head and spine and this showed metastatic disease in 7 patients. One of these patients had supratentorial metastases only (Chang stage M2), the other 6 patients had spinal metastases (Chang stage M3). All patients with localised disease on MRI had lumbar cerebral spinal fluid taken either at diagnosis

or more than 14 days post surgery. One patient without metastatic disease on MRI had tumour cells in the cerebral spinal fluid (Chang stage M1) giving 8 patients in the metastatic group (Chang stages M1 to M3). Where bone marrow aspirates and trephines were performed on the patients with metastatic disease, the samples did not show any evidence of infiltration with medulloblastoma.

The patients ranged in age from 1 to 15 years with 6 of them being under 5 years of age at diagnosis. All patients underwent surgery to resect the primary tumour and the diagnosis of medulloblastoma was made on histopathology. 14 had classic medulloblastoma and 2 patients had a large cell anaplastic medulloblastoma, one of whom had metastatic disease and the other had a localised tumour. All patients had adjuvant treatment with chemotherapy and radiotherapy. Those over 5 years of age had craniospinal radiotherapy, whilst the younger children had focal radiotherapy. Craniospinal radiotherapy doses (24–35 Gy) were lower for those with localised disease than those with metastatic disease (40 Gy). Younger children were treated on a regime with intensive induction chemotherapy prior to focal radiotherapy (45 Gy) followed by conventional chemotherapy. Since the children were not treated according to a common protocol, variations in treatment will strongly influence any formal analysis of survival which is not attempted in this paper.

3.2. *Histopathology*

Between 1 and 9 (mean 4) slides were analysed from each tumour which equated to a range of 0.25–16 cm^2 (mean 3 cm^2) analysed. Ki67 values ranged from 12% to 70% with no significant difference between the metastatic and localised tumours (see Table 1). Levels of necrosis ranged between 0% and 20%. Thirteen tumours had a caspase3 value of less than 10%, whilst the other three had values of 35%, 50% and 55%. Again there were no significant differences in the levels of necrosis, caspase3 uptake or viable tumour fraction between the metastatic and localised tumours (see Table 1).

3.3. *Magnetic resonance imaging and spectroscopy*

A comparison of primary tumour volumes showed that the localised tumours were significantly larger than the metastatic tumours ($p = 0.01$), Table 1. In Fig. 2, an average MR spectrum derived from the patients with localised medulloblastoma is compared with a spectrum from patients with metastatic disease. Inspection of these spectra shows that the total choline (at 3.2 ppm) is increased and mobile lipids (1.3 and 0.9 ppm) are decreased in the metastatic compared with the localised group. Analysis of the spectra by LCModel confirms that the ratio of total choline to total lipid concentration is significantly greater in the metastatic group ($p = 0.01$) with the choline concentration being raised ($p = 0.03$) and the lipid levels being reduced ($p = 0.04$) (Table 1). The LCModel analysis also shows that the levels of lactate are significantly higher in the non-metastatic group ($p = 0.04$) whilst there is a tendency towards lower creatine ($p = 0.09$) and taurine ($p = 0.07$) levels in these tumours. There was no significant difference in the concentrations of any of the metabolites between those >5 years and <5 years of age. Principal component analysis was undertaken to determine the variability in MRS profile in the patient cohort (Fig. 3). This shows that there is a good separation between metastatic and localised tumours with a greater variability in the localised group.

The immunohistochemical staining with Ki67 gives a measure of proliferating cells and may be used as a surrogate for tumour growth. In Fig. 4 it is seen that there is a positive correlation between Ki67 and tCho, which is significant for the whole group of tumours but is stronger for localised tumours than for metastatic tumours. There was no correlation between mobile lipid levels and histopathological parameters frequently used to determine necrosis/apoptosis versus viable tumour fraction. A highly significant correlation between log(lipids/tCho) and tumour volume was found and this was due entirely to a strong correlation in the localised group of tumours (Fig. 5).

Table 1 – A statistical comparison between metastatic and non-metastatic medulloblastoma for various clinical and histopathological characteristics along with metabolite concentrations measured using LCModel

	Metastatic (M1–M3)		Nonmetastatic (M0)		P value
	Mean	SD	Mean	SD	
Characteristic					
Age (yrs)	9.0	4.1	5.4	3.3	0.07
Tumour volume (ml)	28	8	42	11	**0.01***
Ki67 index	37%	15%	38%	20%	0.46
Viable tumour fraction	0.81	0.20	0.89	0.16	0.46
Metabolite					
Total choline (mMol)	3.9	1.2	2.5	1.2	**0.03***
Lipids (1.3 ppm + 0.9 ppm) (mMol)	27.2	10.2	55.5	35.3	**0.04***
Total choline/lipids	0.16	0.06	0.07	0.07	**0.01***
Lactate (mMol)	1.4	0.8	4.1	3.3	**0.04***
Creatine (mMol)	3.7	1.0	2.3	2.0	0.09
Taurine (mMol)	1.9	0.6	1.1	1.0	0.07
N-acetyl-aspartate (mMol)	0.3	0.2	0.2	0.2	0.31
Myo-inositol (mMol)	4.6	2.0	4.7	3.7	0.92

P values given are for Student's *t*-test with a two-tailed distribution.

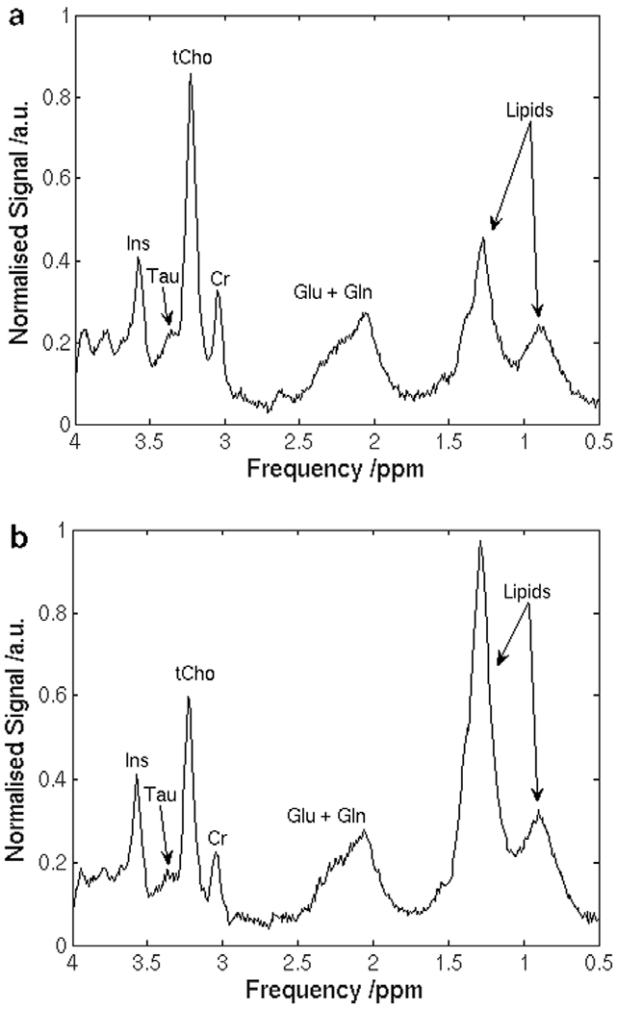

Fig. 2 – Plots showing the mean MR spectra of (a) the metastatic medulloblastoma group (N = 8) and (b) the non-metastatic medulloblastoma group (N = 8). The spectra were processed using LCModel and averaged after subtracting the baseline and normalising with respect to the water reference signal in each case.

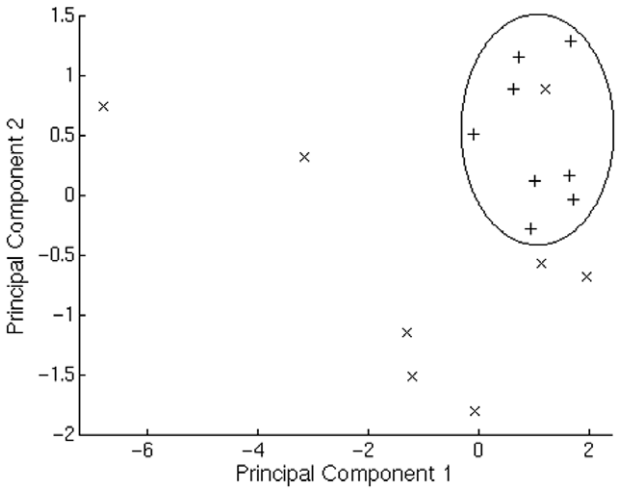

Fig. 3 – Plot of principal component 1 against principal component 2 resulting from a principal components analysis of the MR spectra of the whole dataset (N = 16) between 0.2 and 4.0 ppm. The + symbols indicate the metastatic medulloblastoma cases and the × symbols represent the non-metastatic medulloblastoma cases. The ellipse is drawn arbitrarily to contain all the metastatic cases.

In no patient was the nearest point of the voxel closer than 5 mm to the scalp. There was no significant difference in distance of the voxels from the scalp between metastatic tumours, non-metastatic tumours and controls. Analysis of the spectra from controls showed an average mobile lipid level of 7 mmol/l compared with 27.2 mmol/l for metastatic and 55.5 mmol/l for non-metastatic tumours.

4. Discussion

Significant differences exist in the metabolite profiles of metastatic compared to localised medulloblastoma at presentation. Metastatic tumours are characterised by higher tCho consistent with increased cell turnover and tumour growth, which is substantiated by a significant positive correlation between tCho and the Ki67 index. The observation of higher mobile lipid levels in the localised tumours may reflect a higher proportion of non-viable tumour in these cases.[17] This finding is consistent with the tendency for localised tumours to have higher lactate and lower creatine levels both of which are associated with anaerobic stress. Taurine is present in both metastatic and localised tumours but there is a tendency to higher levels in the metastatic tumours, consistent with previous findings in neuroblastoma that taurine is a marker for more aggressive subtypes in neural tumours.[26]

In addition to demonstrating that there is a significant difference in the average values of specific metabolites in the metastatic and localised tumours, it is important to ascertain the intra-group variability of the metabolite profiles. PCA reveals a good separation of the metastatic from localised tumours with only one localised tumour falling within the metastatic group. It is also seen that the variability of the metabolite profiles is greater in the localised group than the metastatic group with the metastatic tumours forming a tight cluster but the non-metastatic tumours being dispersed. This implies that the downstream effects of the genetic alterations in metastatic tumours are more consistent than those in localised tumours in which many pathways to tumourigenesis have been identified.[5]

If the localised tumours are considered alone, some of the tumours are seen to possess metabolite profiles similar to those of the metastatic group. One of the localised cases falls within the metastatic group, this patient is alive on treatment. Two other localised cases have metabolite profiles similar to metastatic cases, both children have subsequently relapsed with metastatic disease suggesting that the metabolite profile can be used to identify those tumours which possess an enhanced ability to metastasis compared to other localised tumours or may have occult metastases at diagnosis.

An interesting finding in this study is that the primary tumours are larger in patients with localised disease. The lower total choline levels found in localised tumours imply that they

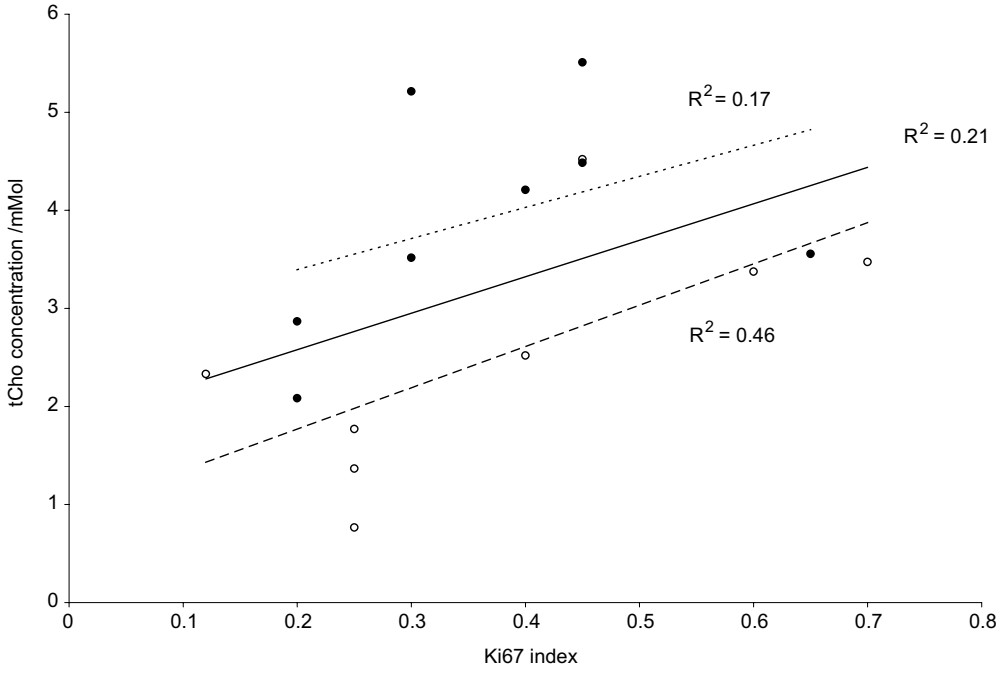

Fig. 4 – Plot of Ki67 labelling index against total choline concentration (phosphocholine, PCh + glycerophosphocholine, GPC) from LCModel analysis for metastatic medulloblastoma (solid circles) and non-metastatic medulloblastoma (open circles). The lines show the correlation within the whole dataset (solid, $R^2 = 0.21$, $P < 0.05$), the non-metastatic group (dashed, $R^2 = 0.46$, $P < 0.05$) and the metastatic group (dashed, $R^2 = 0.17$, not significant).

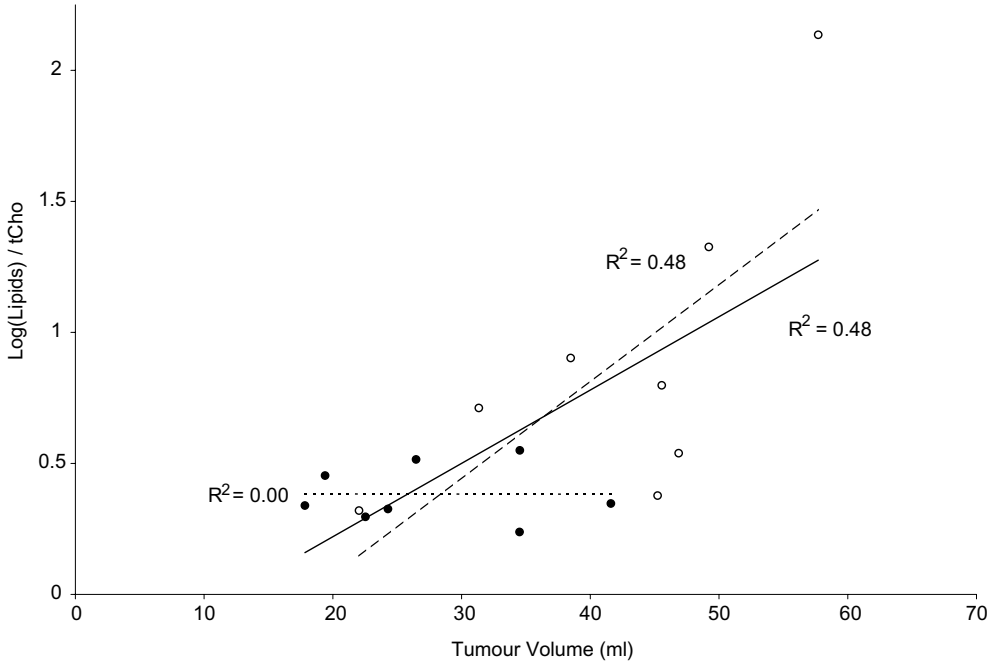

Fig. 5 – Plot of tumour volume at time of diagnosis as measured from MRI scan against the ratio of the log of the lipid concentration (peak at 1.3 ppm + peak at 0.9 ppm) to the total choline concentration from the LCModel analysis for metastatic medulloblastoma (solid circles) and non-metastatic medulloblastoma (open circles). The lines show the correlation within the whole dataset (solid, $R^2 = 0.48$, $P < 0.005$), the non-metastatic group (dashed, $R^2 = 0.48$, $P < 0.05$) and the metastatic group (dashed, $R^2 = 0.00$).

are growing more slowly and the high lipid and lactate levels indicate a degree of anaerobic stress and loss of viability which increase as the tumour grows outstripping angiogenesis. This implies that localised tumours have a lower metastatic potential rather than simply having been diagnosed earlier. Conversely, the metastatic tumours have primaries which are

smaller, with high total choline levels and lower lipid and lactate levels. This implies that these tumours grow rapidly and metastasis early when the tumour is still small and a high proportion of the cells are metabolically active.

The absence of a correlation between mobile lipids and viable tumour fraction in this study could result from the heterogeneity of these features within the tumour combined with limited histopathological sampling of each tumour. MRS determines metabolite concentrations averaged across a voxel of at least 3.4 cm^3, which is large compared with the size of each biopsy. This possibility could be further explored using *in vitro* magic angle spinning MRS, where small tissue samples (less than 5 mg) can be analysed and left intact allowing histopathology to be performed on the same sample.[27] Alternatively, the lack of correlation between mobile lipids and viable tumour fraction may be due to the inability of the current histopathological measures to detect early changes associated with loss of cell viability. *In vitro* studies have shown that the mobile lipids measured by MRS reside in lipid droplets within cells as well as in necrotic tissue[22] and such cells may still be viable. Indeed, it has been noted previously that viable tumour could be found in areas of tumour with high lipids on MRS.[28] Where levels of necrosis are low, as in this study, the MRS mobile lipid levels are dominated by the intracellular lipids and a reliable histopathological correlate of this cellular lipid accumulation has not yet been developed.

This study reveals that significant differences exist in the metabolite profiles of metastatic versus localised medulloblastoma. Importantly, we provide preliminary evidence that localised tumours with similar metabolite profiles to metastatic cases are at increased risk of relapse. In order to confirm this hypothesis and to establish metabolite profiles as an independent prognostic marker, we now need to incorporate MRS in prospective clinical trials with larger numbers of patients treated in a uniform manner. Such studies need to be carried out on a multicentre basis. In the UK, we are pursuing this strategy through the Children's Cancer and Leukaemia Group.[29]

Conflict of interest statement

None declared.

Acknowledgements

A.C.P. holds a Department of Health Clinician Scientist Award which also funds S.L. N.P.D. and K.N. are in part funded by the European Union Framework 6 Integrated Project eTUMOUR FP6-2002-LIFESCIHEALTH 503094. The project was also funded in part by the Alistair Wainwright & Joe Foote Fund and the Birmingham Children's Hospital Research Foundation.

REFERENCES

1. Ellison DW, Onilude OE, Lindsey JC, et al. Beta-catenin status predicts a favourable outcome in childhood medulloblastoma: the United Kingdom Children's Cancer Study Group Brain Tumour Committee. *J Clin Oncol* 2005;**23**:7951–7.
2. Gilbertson RJ, Pearson AD, Perry RH, Jaros E, Kelly PJ. Prognostic significance of the c-erbB-2 oncogene product in childhood medulloblastoma. *Br J Cancer* 1995;**71**:473–7.
3. Grotzer MA, Janss AJ, Fung K, et al. Trk C expression predicts good clinical outcome in primitive neuroectodermal brain tumours. *J Clin Oncol* 2000;**18**:1027–35.
4. Pomeroy SL, Tomayo P, Gaasenbeek M, et al. Prediction of central nervous system embryonal tumour outcome based on gene expression. *Nature* 2000;**415**:436–42.
5. Thompson MC, Fuller C, Hogg TL, et al. Genomics identifies medulloblastoma subgroups that are enriched for specific genetic alterations. *J Clin Oncol* 2006;**24**:1924–31.
6. Panigraphy A, Krieger MD, Gonzalez-Gomez I, et al. Quantitative short echo time 1H MR spectroscopy of untreated paediatric brain tumours: pre-operative diagnosis and characterisation. *AJNR* 2006;**27**:560–72.
7. Preul MC, Caramanos Z, Collins DL, et al. Accurate, noninvasive diagnosis of human brain tumours by using proton magnetic resonance spectroscopy. *Nat Med* 1996;**2**:323–5.
8. Astrakas LG, Zurakowski D, Tzikka AA, et al. Noninvasive magnetic resonance spectroscopic imaging biomarkers to predict the clinical grade of pediatric brain tumors. *Clin Cancer Res* 2004;**10**:8220–8.
9. Girard N, Wang ZJ, Erbetta A, et al. Prognostic value of proton MR spectroscopy of cerebral hemisphere tumours in children. *Neuroradiology* 1998;**40**:121–5.
10. Li X, Jin H, Lu Y, et al. Identification of MRI and 1H MRSI parameters that may predict survival for patients with malignant gliomas. *NMR Biomed* 2004;**17**:10–20.
11. Vaidya SJ, Payne GS, Leach MO, Pinkerton CR. Potential role of magnetic resonance spectroscopy in assessment of tumour response in childhood cancer. *Eur J Cancer* 2003;**39**:728–35.
12. Warren KE, Frank JA, Black JL, et al. Proton magnetic resonance spectroscopic imaging in children with recurrent primary brain tumours. *J Clin Oncol* 2000;**18**:1020–6.
13. Preul MC, Caramanos Z, Leblanc R, Villemure JG, Arnold D. Using pattern analysis of in vivo proton MRSI data to improve the diagnosis and surgical management of patients with brain tumours. *NMR Biomed* 1998;**11**:192–200.
14. Catalaa I, Henry R, Dillon WP, et al. Perfusion, diffusion and spectroscopy values in newly diagnosed cerebral gliomas. *NMR Biomed* 2006;**19**:463–75.
15. Howe FA, Barton SJ, Cudlip SA, et al. Metabolic profiles of human brain tumours using quantitative in vivo proton magnetic resonance spectroscopy. *Mag Res Med* 2003;**49**:223–32.
16. Peet A, Garala P, MacPherson L, Natarajan K, Sgouros S, Grundy R. Mobile lipids detected by short echo time 1H magnetic resonance spectroscopy correlate with malignancy in childhood brain tumours. *Neurooncology* 2004;**6**:471.
17. Lindskog M, Kogner P, Ponthan F, et al. Non invasive estimation of tumour viability in a xenograft model of human neuroblastoma with proton magnetic resonance spectroscopy (^{1}H MRS). *Br J Cancer* 2003;**88**:478–85.
18. Ronen SM, Jackson LE, Beloueche M, Leach MO. Magnetic resonance detects changes in phosphocholine associated with Ras activation and inhibition in NIH 3T3 cells. *Br J Cancer* 2001;**84**:691–6.
19. Glunde K, Jie C, Bhujwaller ZM. Molecular causes of aberrant choline phospholipids metabolism in breast cancer. *Cancer Res* 2004;**64**:4270–6.
20. Rodriguez-Gonzalez A, de Molina A, Fernandez F, et al. Inhibition of choline kinase as a specific cytotoxic strategy in oncogne-transformed cells. *Oncogene* 2003;**22**:8803–12.

21. Blankenberg FG, Katsikis PD, Storrs RW, et al. Quantitative analysis of apoptotic cell death using proton nuclear magnetic resonance spectroscopy. *Blood* 1997;**89**:3778–86.
22. Barba I, Cabanas ME, Arus C. The relationship between nuclear magnetic resonance visible lipids, lipid droplets and cell proliferation in cultured C6 cells. *Cancer Res* 1999;**59**:1861–8.
23. Sgouros S, Goldin HJ, Hockley AD, Wake MJC, Natarajan K. Intracranial volume change in childhood. *J Neurosurgery* 1999;**91**:610–6.
24. Provencher SW. Estimation of metabolite concentrations from localized in vivo proton NMR spectra. *Magn Reson Med* 1993;**30**:672–9.
25. Frahm J, Hanefeld F. Localized proton magnetic resonance spectroscopy of cerebral metabolites. *Neuropediatrics* 1996;**27**:64–9.
26. Peet AC, Wilson M, Levine B, McConville C, Grundy R. ^{1}H NMR spectroscopy identifies differences in choline metabolism related to the MYCN oncogene in neuroblastoma. *Proc Intl Soc Mag Reson Med* 2005;**13**:2489.
27. Barton SJ, Howe FA, Tomlins AM, et al. Comparison of in vivo ^{1}H MRS of brain tumours with 1H HR-MAS spectroscopy of intact biopsy samples in vitro. *Magma* 1999;**8**:121–8.
28. Negendank W, Sauter R. Intratumoral lipids in proton MRS in vivo in brain tumours: experience of the Siemens cooperative clinical trial. *Anticancer Res* 1996;**16**:1533–8.
29. Peet AC, Leach MO, Pinkerton CR, Price P, Williams SR, Grundy RG. The development of functional imaging for the diagnosis, management and understanding of childhood brain tumours – an EPSRC workshop. *Paediatric Blood Cancer* 2005;**44**:103–13.